Spatio-temporal assessment of beech growth in relation to climate extremes in Slovenia – An integrated approach using remote sensing and tree-ring data

Mathieu Decuyper[a,d,m,*], Roberto O. Chávez[b], Katarina Čufar[e], Sergio A. Estay[c,i], Jan G.P.W. Clevers[a], Peter Prislan[f], Jožica Gričar[f], Zalika Črepinšek[g], Maks Merela[e], Martin de Luis[h], Roberto Serrano Notivoli[j], Edurne Martinez del Castillo[h], Danaë M.A. Rozendaal[a,d,k,l], Frans Bongers[d], Martin Herold[a], Ute Sass-Klaassen[d]

[a] Laboratory of Geo-Information Science and Remote Sensing, Wageningen University, P.O. Box 47, Wageningen 6700 AA, the Netherlands
[b] Laboratorio de Geo-información y Percepción Remota, Instituto de Geografía, Pontificia Universidad Católica de Valparaíso, Valparaíso, Chile
[c] Universidad Austral de Chile, Instituto de Ciencias Ambientales y Evolutivas, Facultad de Ciencias, Valdivia, Chile
[d] Forest Ecology & Management, Wageningen University, P.O. Box 47, Wageningen 6700 AA, the Netherlands
[e] Department of Wood Science and Technology, Biotechnical Faculty, University of Ljubljana, Ljubljana, Slovenia
[f] Slovenian Forestry Institute, Ljubljana, Slovenia
[g] Department of Agronomy, Biotechnical Faculty, University of Ljubljana, Ljubljana, Slovenia
[h] University of Zaragoza, Department of Geography and Regional Planning, Zaragoza, Spain
[i] Center of Applied Ecology and Sustainability (CAPES). Pontificia Universidad Católica de Chile, Santiago, Chile
[j] Estación Experimental de Aula Dei (EEAD-CSIC), Spanish National Research Council, Zaragoza, Spain
[k] Plant Production Systems Group, Wageningen University, P.O. Box 430, Wageningen 6700 AK, the Netherlands
[l] Centre for Crop Systems Analysis, Wageningen University, P.O. Box 430, Wageningen 6700 AK, the Netherlands
[m] World Agroforestry (ICRAF), P.O. Box 30677-00100 GPO, Nairobi, Kenya

ARTICLE INFO

ABSTRACT

Climate change is predicted to affect tree growth due to increased frequency and intensity of extreme events such as ice storms, droughts and heatwaves. Yet, there is still a lot of uncertainty on how trees respond to an increase in frequency of extreme events. Use of both ground-based wood increment (i.e. ring width) and remotely sensed data (i.e. vegetation indices) can be used to scale-up ground measurements, where there is a link between the two, but this has only been demonstrated in a few studies. We used tree-ring data together with crown features derived from the Moderate Resolution Imaging Spectroradiometer (MODIS) to assess the effect of extreme climate events on the growth of beech (Fagus sylvatica L.) in Slovenia. We found evidence that years with climate extremes during the growing season (drought, high temperatures) had a lower ring width index (RWI) but we could not find such evidence for the remotely sensed EVI (Enhanced Vegetation Index). However, when assessing specific events where leaf burning or wilting has been reported (e.g. August 2011) we did see large EVI anomalies. This implies that the impact of drought or heatwave events cannot be captured by EVI anomalies until physical damage on the canopy is caused. This also means that upscaling the effect of climate extremes on RWI by using EVI anomalies is not straightforward. An exception is the 2014 ice storm that caused a large decline in both RWI and EVI. Extreme climatic parameters explained just a small part of the variation in both RWI and EVI by, which could indicate an effect of other climate variables (e.g. late frost) or biotic stressors such as insect outbreaks. Furthermore, we found that RWI was lower in the year after a climate extreme occurred in the late summer. Most likely due to the gradual increase in temperature and more frequent drought we found negative trends in RWI and EVI. EVI maps could indicate where beech is sensitive to climate changes and could be used for planning mitigation interventions. Logical next steps should focus on a tree-based understanding of the short -and long-term effects of climate extremes on tree growth and survival, taking into account differential carbon allocation to the crown (EVI) and to wood-based variables. This research highlights the value of an integrated approach for upscaling tree-based knowledge to the forest level.

* Correspondence at: Laboratory of Geo-information Science and Remote Sensing Droevendaalsesteeg 3Gaia, buildingnumber 1016708 PB Wageningen, The Netherlands
  E-mail address: mathieu.decuyper@wur.nl (M. Decuyper).

1. Introduction

Many studies indicate that at Northern latitudes the effect of climate change (i.e. warming due to increasing CO_2 levels) prolongs the growing season of trees (Badeck et al., 2004; Menzel, 2002; Nabuurs et al., 2002; Nemani et al., 2003). Although increasing CO_2 levels enable trees to use water more efficiently, their growth and biomass production may be curbed by increased climate-induced water shortage (Bréda et al., 2006; Fonti et al., 2013), heat stress (Bréda et al., 2006; Ciais et al., 2005), or increased respiratory demands (McDowell et al., 2008).

Summer droughts are common in Europe and are known to reduce wood formation (i.e. tree-ring width) for species such as Scots pine (*Pinus sylvestris* L.) (Gruber et al., 2010) and beech (*Fagus sylvatica* L.) (Ciais et al., 2005; Čufar et al., 2008a; Di Filippo et al., 2007; Giagli et al., 2016; Prislan et al., 2013; Scharnweber et al., 2011; van der Werf et al., 2007). However, recent studies also indicated that at some sites precipitation is not necessarily a limiting factor for beech growth (Prislan et al., 2018). Moreover, beech can show plastic growth reactions, such as in 2003, when beech from a site in the Netherlands temporarily stopped growing under summer drought followed by growth activation under improved conditions later in the growing season (van der Werf et al., 2007). Also the influence of temperature on beech growth can differ depending on timing and site conditions (Čufar et al., 2008b; Di Filippo et al., 2007; Fischer and Neuwirth, 2013; Prislan et al., 2019; van der Werf et al., 2007). Above-average summer temperature can have a negative effect on growth at lowland sites, where it can induce drought stress due to enhanced evapotranspiration under limited water resources but positively affects growth at high elevation sites where growth is not water-limited (Wu et al., 2015). This implies that the impact of expected climate changes on tree growth depends on the interplay of specific site conditions defining the baseline for resource availability (water, nutrients, energy/light) and prevailing climate factors defining the amplitude of variation in resource availability for each year. Tree growth at a given site is adapted to these amplitudes, and tree growth varies according to changes in resource availability as modulated by annually changing climate conditions. During years with extreme climate conditions, site-specific amplitudes of resource availability are crossed and tree growth declines, sometimes for several years. Besides these resource-related effects, which affect trees through tree physiology, i.e. the water and carbon cycle (Hacket-Pain et al., 2015), growth can also be affected by (mechanical) injury of tree organs, i.e. suffocating roots through flooding, burned leaves during heatwaves or broken branches through (ice) storms (Marenče, 2015). Tree growth is thus the product of intact tree organs and the complex tree physiological processes, which are largely influenced by climate-related changes in resource availability (Norman et al., 2016; Sass-Klaassen et al., 2016).

Assessment of tree growth can be done at tree level, e.g. by applying dendrochronological methods or at stand or site level with the aim to detect total biomass of trees or forest stands by applying various remote sensing techniques (Avitabile et al., 2015). Vegetation indices from satellites can be used as a proxy for forest health and biomass. Tree-centred measurement methods such as tree-ring research and xylogenesis are unique tools to assess and understand long-term climate-growth relationships. However, the fact that they are tree centred implies that information is always collected for specific sites or areas which, due to local effects of climate or soil characteristics, can often not be considered representative for large-scale assessments (Norman et al., 2016). Conversely, remote sensing techniques can be used for large-scale inventory of forest health (Coops et al., 2009). The combination of both methods can be used to assess factors behind susceptibility of forest areas to extreme climate events by mapping forest areas that have been affected by past extreme climate events and to investigate their specific site and tree characteristics. Several studies indicated the potential of remote-sensing indices to detect the impact of drought or heat waves on forest populations (Hlásny et al., 2015; Vicca et al., 2016). However, due to the relatively coarse spatial resolution of a particular sensor (30–250 m for sensors that have longer time series available) and depending on the forest structure, grid cells often integrate signals from trees of different species or trees and undergrowth, unless large, homogeneous forest patches are present (Deshayes et al., 2006). Furthermore, vegetation indices sensitive to the green biomass of the canopy provide an efficient indicator of photosynthetic activity and tree productivity, but until now only few studies attempted to link tree-ring width as direct growth indicator of the stem with remote sensing derived indices (Babst et al., 2018; Bunn et al., 2013; Decuyper et al., 2016). Photosynthetic activity determines the amount of carbohydrates available for physiological processes including wood formation. Thus, leaf phenology is intrinsically linked to cambial phenology and, therefore, to wood formation. Yet, it is not clear how remotely-sensed indices related to chlorophyll pigments in the leaves and the amount of leaves relate to intra- and inter-annual dynamics in wood formation. A combination of remotely sensed indicators of photosynthetic activity and field-based tree-ring analyses can fill this gap. By focussing on years with extreme climate conditions the approach can be tested as it is assumed that a strong reduction of resources like water (drought) or a direct impact of high temperature
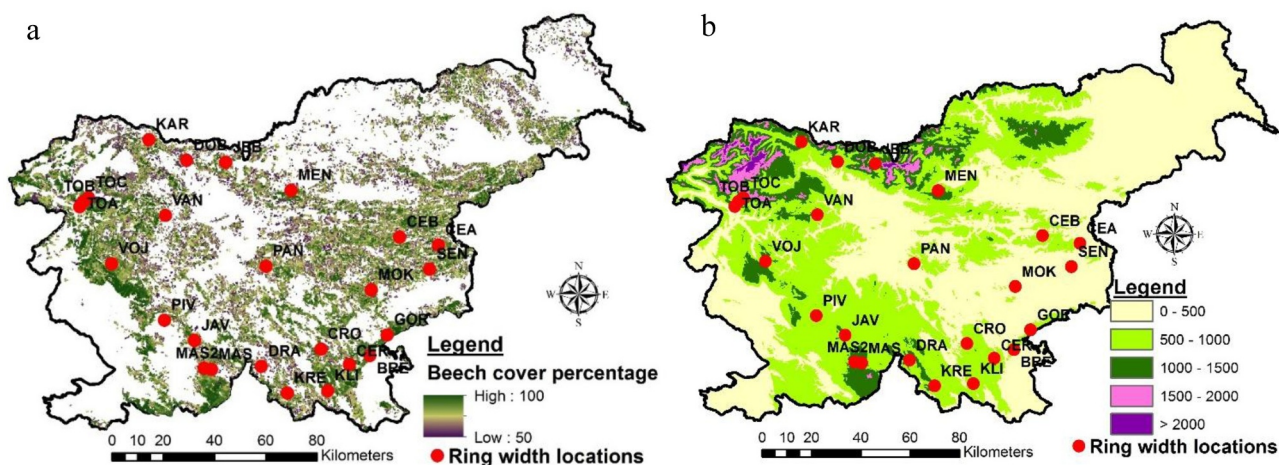

Fig. 1. Maps of Slovenia with: a) beech cover map where white areas represent < 50% and colored ones 50–100% of beech cover (source: Slovenian Forest Service), and b) elevation map in m.a.s.l. Red dots mark dendrochronological sites (referred to with abbreviations).(For interpretation of the references to colour in this figure legend, the reader is referred to the web version of this article.)

through burning or wilting of leaves (heatwave) or an ice storm causing breaking of branches will impact both the canopy (in terms of the Enhanced vegetation Index, EVI) and stem growth (through the ring width index, RWI), in that specific year.

In this study, we assess the effect of climate extreme events on the growth of beech in Slovenia, both from a tree-ring width (tree stem) and remote sensing (forest canopy) perspective. Although the distribution of beech has been generally increasing recently, this species has been affected by adverse climate effects, like ice damage (2014), heat waves and droughts (2003, 2011, 2013 and 2015) (Marenče, 2015; Kozjek et al., 2017; Slovenian Forest Service, 2017). This is why special emphasis is put on the effect of the fast succession of these climate extreme events on beech growth at different forest sites across Slovenia. Based on the results an attempt will be made to upscale local effects on RWI observed from specific sites to all beech forest stands in Slovenia using remote sensing techniques.

Specifically, we addressed the following questions:

- How do climate variables and specifically extreme climate events affect beech in terms of photosynthetically active canopy (EVI) and tree ring width index (RWI) at different forest sites across Slovenia?
- Are there changes in (long-term) growth trends (1961–2016 for RWI and 2001–2017 for EVI) as a consequence of rising temperature and climate extreme events?
- Is the response in tree-ring width linked to a response in canopy condition, and can we therefore upscale observed local effects on ring width index (RWI) to regional effects using remote sensing data (EVI)?

2. Materials and methods

2.1. Study area and species description

Slovenia is characterized by temperate forests covering about 58% of the territory (Slovenian Forest Service, 2017) (Fig. 1). With 346 million cubic meters of growing stock, the Slovenian forests have an important economic value. In fact, European beech (*Fagus sylvatica* L.) represents 32% of the wood stock (Slovenian Forest Service, 2017). Beech as the leading forest species, grows on a large variety of sites in different biogeographical zones of the country with different climatic regimes. Beech grows in monospecific stands, favouring the retrieval of a pure signal from satellite images, and also its leaves contain high amounts of lignin, limiting understory growth, which reduces the probability of having a mixed signal (Mölder et al., 2008).

A national beech cover map based on the National Forest Inventory (NFI) (Slovenian Forest Service, 2017) was created (Fig. 1a). Areas with a beech cover of < 50% were removed from the analysis to avoid influence of other tree species or land uses on remote sensing indices. Using the R software (R Core Team, 2019), the vector polygons of the beech map were rasterized and resampled to fit the Moderate Resolution Imaging Spectroradiometer (MODIS) product of 250 m grid size (see Section 2.4). Only MODIS pixels with ≥ 50% of the area covered by beech polygons were included in this study.

2.2. Dendrochronological data

Dendrochronological ring width index (RWI) data for 25 sites were included (Fig. 1) mainly from previous studies (e.g. Čufar et al., 2008b; Prislan et al., 2018, 2013) with different elevations (Fig. 1b). Sample size varied from 5 - 32 trees per site, with an age between 61 and 271 years. RWI time series vary in length, ending between 2001–2016 due to the time of sampling (Appendix A). Detailed descriptions of sampling and sample preparation can be found in Čufar et al. (2008b); Čufar et al. (2014); Prislan et al. (2018); Prislan et al. (2013)(Prislan et al., 2018). To correct for ontogenetic effects, all raw ring width series were standardized using regional curve standardizations (RCS) in the ARSTAN 6.05P programme (Cook, 1985). RCS is an age-dependent composite method and involves dividing the size of each tree ring by the value expected from its cambial age. A biweight robust mean was applied to detrended tee-ring indices to develop the site chronologies. To evaluate
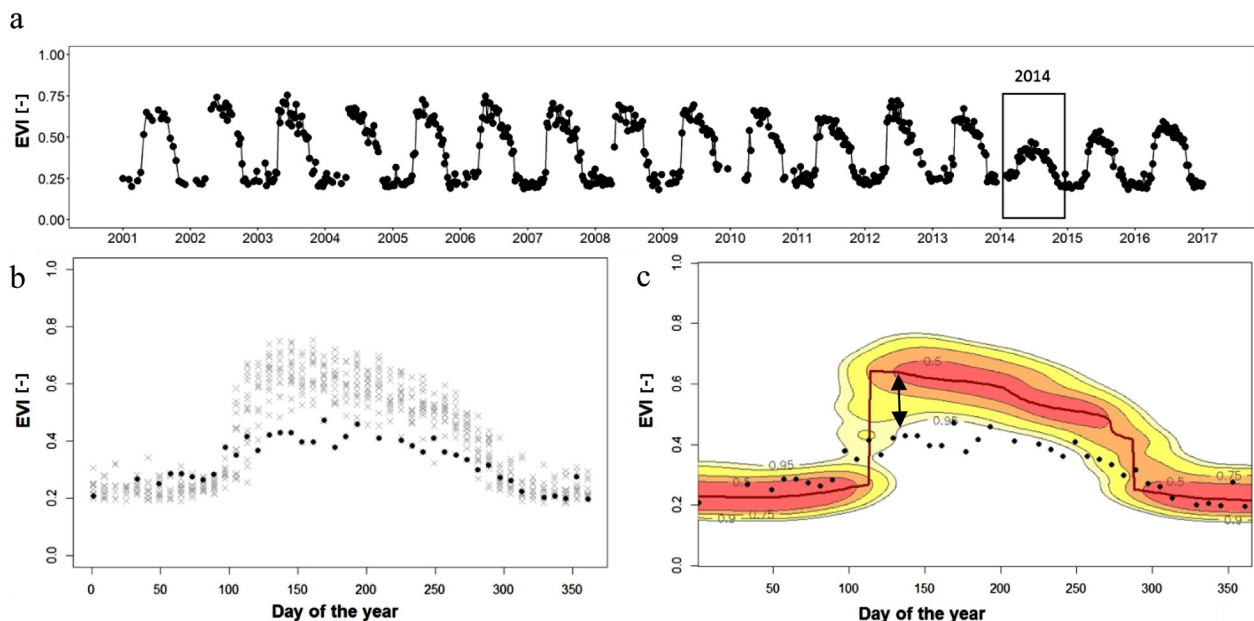

Fig. 2. Calculation of the Enhanced Vegetation Index (EVI) anomalies for a single 250 m pixel of *Fagus sylvatica* forest. a) The full time series of 8-day composites of EVI values is extracted for the given pixel. The black box shows the growing season 2014 (a year with a severe ice storm) to be analysed. b) The EVI values from all growing seasons (grey x), except for the growing season to be analysed (2014 in black circled dots), are used to calculate the reference EVI curve (showing the seasonal behaviour of this forested pixel) using kernel density estimation. c) The probability (red and yellow shades) of an EVI value occurring at a given day of the year is calculated: the dark red line (maximum probability) shows the reference EVI phenological curve for this forested pixel. The difference between the dark red line (reference) and the black dots (measured values in 2014), the EVI anomaly (black arrow), is then used to account for a disruption.(For interpretation of the references to colour in this figure legend, the reader is referred to the web version of this article.)

uncertainty in the chronologies, the express population signal (EPS) were calculated. EPS is an estimate of the chronology's ability to represent the signal strength of a chronology on a theoretically infinite population. The portion of the chronologies with expressed population signal (EPS) values exceeding 0.85 were used for further analysis (Wigley et al., 1984). The RWI series of individual trees were averaged into site chronologies.

2.3. Remote-sensing data

The entire 16-days MODIS vegetation indices catalogue from the Terra (product MOD13Q1) and Aqua (MYD13Q1) satellites was used in this study. These satellites acquire global images on a daily basis and, in order to avoid data gaps due to clouds and other atmospheric contamination, they are composed within a temporal window of 16 days. From this product, the Enhanced Vegetation Index (EVI) was selected due to the sensitivity to leaf phenological changes (Huete et al., 2002; White et al., 2014). Other useful MODIS products are the GPP (Gross Primary Production) and LAI (Leaf Area Index), but the coarser spatial resolution (i.e. 500 m) made them less suitable for this study. Combining the MODIS Terra and Aqua satellite data, a time series of 768 MODIS EVI layers was obtained, spanning from 2000 until 2017. Since the vegetation indices (VI) algorithm of each of the two satellites is generated as a 16-day composite, and they are eight days apart, we compiled a time series with a temporal resolution of 8 days. All the scenes were pre-processed using the quality flags provided within the MODIS vegetation indices product using the 'raster' R package (Hijmans and van Etten, 2012). Based on these quality flags, all pixels with clouds, cloud shadows, water, snow, ice, and images with a high level of aerosols were neglected.

Potential detrimental effects on the canopy condition (reduction of photosynthetically active foliage) were studied by means of EVI anomalies using the "npphen" R package (Chávez et al., 2017). This is a probabilistic approach for phenological estimation and anomaly detection which has been successfully applied to study forest disturbances (Bowman et al., 2019; Chávez et al., 2019; Estay et al., 2019). As illustrated in Fig. 2, for each 250 × 250 m MODIS pixel, the EVI time series for the period 2001–2017 was extracted, resulting in a 768 time step series in the most favourable case (i.e. no clouds or cloud shadows) (Fig. 2a). The time series were sorted by the day of the year (DOY) per year to calculate the reference phenological curve (Fig. 2b). Using all available EVI values (i.e. 46 per year), the maximum probability of having a given EVI value at a given DOY was calculated (dark red line in Fig. 2c). Probabilities of having certain EVI values at different DOY were calculated using the 'npphen' R package (Chávez et al., 2017).

An iterative leave-one-out process was applied to calculate EVI anomalies for the complete time series. In this process, a given year (e.g. 2014, Fig. 2) is left out and the reference annual phenological cycle is then estimated using the remaining years (Fig. 2b). Then, the EVI anomaly for the given year is calculated by subtracting the reference values from the measured values of that year. Positive EVI anomalies indicate a higher photosynthetic activity than normal (greening) of the vegetated land surface while negative anomalies show a lower photosynthetic activity (browning). All pixels of Slovenia together provide a national EVI anomaly map, and 46 anomaly maps were obtained per year, i.e. 768 maps for the period 2001–2017.

Since the aim is to relate the anomaly data to monthly climate parameters, the 8-day resolution EVI anomaly data were averaged per month. To assess possible relations between the annual RW data, average EVI anomaly within the growing season (i.e. June-September) was calculated.

2.4. Climate data and models

Current climate grids are limited in resolution and do not use most of the local climate stations. Therefore, we developed a higher spatial resolution climate grid especially for this study. Daily precipitation and average temperature grids were generated using 491 weather stations covering the whole study area. The stations ranged in altitude from 2 to 2514 m.a.s.l. for the period 1961–2017. The reconstruction for each station was made in two steps (methodology based on: Serrano-Notivoli et al., 2019, 2017b): (1) we flagged and removed unreliable records, and (2) we filled in missing values based on the filtered dataset resulting from the previous step as follows. A grid was created with a cell size of 1 km. To obtain estimated values of temperature for each grid cell, multiple logistic regressions (MLR) were used to compute reference values using altitude, latitude, and longitude as covariates, while generalized linear models (GLM) were used to estimate daily temperature values with same predictors. Daily precipitation for each point of the grid was estimated using two reference values based on the 10 nearest observations on the corresponding day: i) a binomial prediction referred to the probability of occurrence of a wet day and, ii) a magnitude prediction referred to the amount of precipitation using MLR. The reconstructed precipitation and temperature were calculated using the "reddPrec" package in R statistical software (Serrano-Notivoli et al., 2017a).From the daily climate grids, we analyzed monthly climate variables: (i) the average maximum temperature (in °C) per month (from here on: temperature); (ii) the total precipitation (in mm) per month; and (iii) the 3-month Standardized Precipitation Index (SPI). The 3-months were used to account for a seasonal drought (Mckee et al., 1993).

In order to not rely only on reported climate extremes (e.g. drought in 2003), we used the same approach as the anomaly identification for the remote sensing data and created monthly anomalies and their probabilities. By using the probabilities, we accounted for site specific differences (e.g. a precipitation anomaly of -100 might have a high probability of being a climate extreme in a wet site, while this might still be within the normal range in a drier site). When a climate extreme occurred during the growing season (April-August), i.e. values falling within the 90–100% probability of the most extreme historical observations, it was marked as an extreme year for testing against RWI. For EVI anomaly data monthly data (June-September) were used. A year was considered 'normal' when the climate parameter ranged between 0 - >90% probability.

2.5. Statistical analysis

We assessed if there were general climate effects on tree growth by modelling the entire RWI (detrended) and EVI series as a function of climate parameters using linear mixed-effect models ("lme4" R-package) (Bates et al., 2014). Climate parameters were included as fixed effects, together with a random intercept per site and an interaction effect of elevation. We also tested random slopes to account for site specific effects. The best model was selected based on Akaike's Information Criterion (AIC). (Burnham and Anderson, 2002). All models performed poorly, since much of the variation cannot be explained by the model (Appendix B).

To capture the effect of climate extreme events, EVI anomaly data and climate parameters were extracted for all sites. The RWI and EVI anomaly data were divided into climate classes (e.g. for precipitation the 3 classes were: dry (negative anomaly with ≥ 90% probability), normal (between 0 and 89% probability) and wet (positive anomaly with ≥ 90% probability).

The Kruskal-Wallis and Pairwise Wilcoxon Rank Sum test were used to test the statistical difference between the RWI and EVI anomaly classes given a certain climate parameter using the "stats" R package (Hollander and Wolfe, 1973).

To test changes in (long-term) growth trends, a Mann Kendall trend test was used to check trends in climate parameters, RWI and EVI (Hipel and McLeod, 1994). We used the general EVI data (i.e. no anomaly data) for the trend analysis. Temporal stationarity was tested by the autocorrelation function (ACF) and if necessary accounted for by

using the "SeasonalMannKendall" function within the R package "Kendall" (Hipel and McLeod, 1994). The Kendall package was also used to test the correlation between EVI and RWI.

3. Results

3.1. Effect of climate extremes on RWI

The climate anomaly and probabilities allowed the separation of climate extreme years from 'normal' years. While some climate extremes were more local in some years (only few sites affected), there are some years indicating large scale droughts (e.g. 1993 and 2003), and high temperatures (e.g. 2003 and 2011). Extremely dry periods (measured by SPI) in the growing season negatively affected the RWI and was significantly different from the other classes ($\chi^2 = 24.824$, $P > 0.001$), while RWI was the highest, but not significantly different from normal years, in exceptionally wet years (Fig. 3a). In Fig. 4, we marked all the years that were extremely dry and wet according to the SPI. Years with low precipitation had in general a lower RWI but this was not significantly different from the RWI in years with normal precipitation. Years with high precipitation did have a higher and significantly different RWI ($\chi^2 = 11.484$, $P = 0.003$ – Fig. 3b). Extreme high temperatures during RW formation had significantly lower RWI compared to growing seasons with normal and colder temperatures ($\chi^2 = 18.881$, $P > 0.001$). Colder temperatures were not different from

normal years in terms of RWI (Fig. 3c). The RWI in years with climate extreme droughts in the late summer - start of autumn (August-October) were lower in the following year according to the SPI probabilities ($\chi^2 = 9.456$, $P = 0.009$). No differences were found in precipitation but years with hotter temperatures in the August-October period had significantly lower RWI, while this was the opposite for colder temperatures ($\chi^2 = 27.551$, $P > 0.001$ - Fig. 3d).

3.2. Effect of climate extremes on EVI anomalies

Since the EVI time-series is shorter, the year 2014 was left out as this was a lagged effect of the ice storm in February and resulted in extremely negative anomalies. Opposite to RWI, the extremely dry periods (measured by SPI) in the growing season did have a significant positive effect on the canopy, with the highest EVI anomalies in the extreme wet years ($\chi^2 = 11.175$, $P = 0.003$). This effect was not found for precipitation (no significant differences), while years with higher temperatures during the growing season had higher EVI anomalies ($\chi^2 = 11.807$, $P > 0.001$).

As mentioned in Section 2.3, Slovenia had several extreme climate events in the last 15 years (2001–2016). There were reports of leaves that burned and wilted during August 2003, 2011 and 2013. Since the boxplots did show large variation, indicating local climate effects or different site conditions, we aimed to locate the affected areas by making anomaly maps for all the areas with beech cover (Fig. 5).
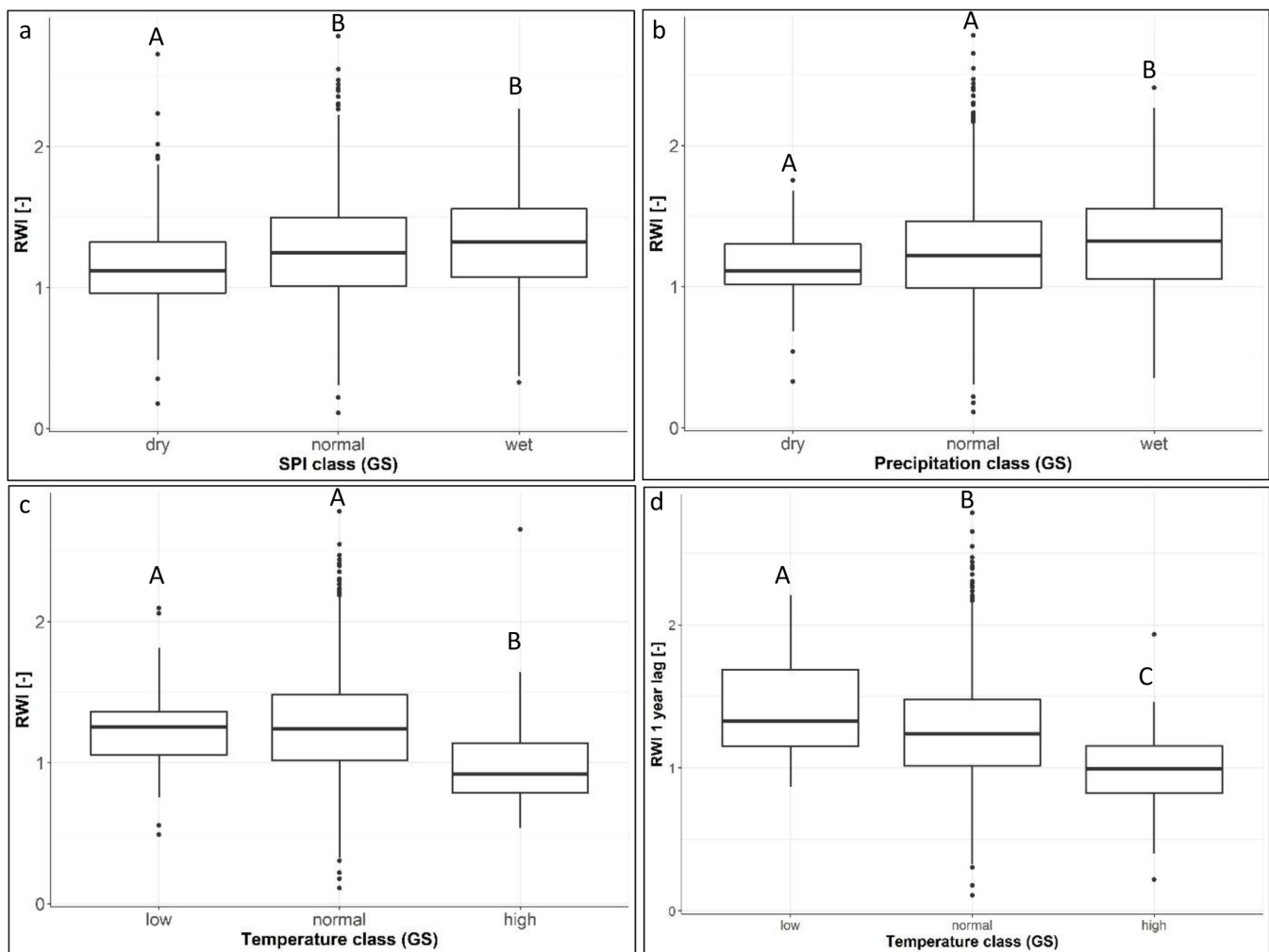

Fig. 3. RWI in years with extreme climate events (i.e. when values are between 90–100% higher or lower than the historical records) versus normal (0 - >90%) years during the growing season (April-July) for a) SPI, b) precipitation and c) temperature. d) RWI in the year following a year with an extremely low, high or normal temperature in the late summer (August-October) of the previous year.
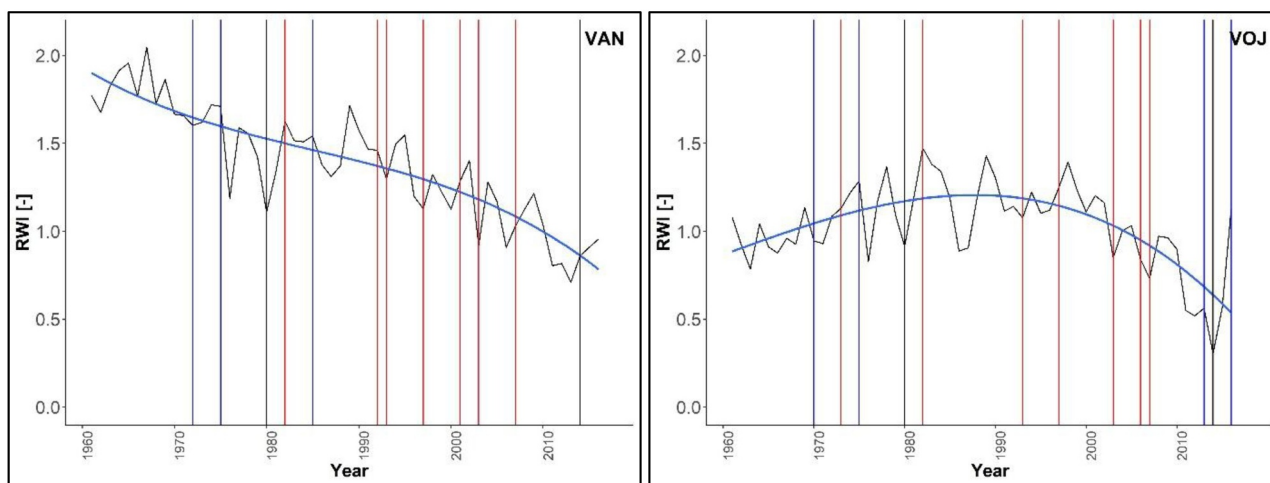
Fig. 4. Example of the RWI of two sites (VAN and VOJ), with the climate extreme years marked. Years with an extremely low and high SPI were respectively marked with red and blue lines, ice storms with a black line.

Fig. 5a shows that mainly the eastern areas were affected by the high temperatures in August 2003. When zooming into one of the sites with a strong negative EVI anomaly (SEN), we can indeed observe a drop in EVI in August (DOY ~220 to ~240), compared to the other years (Fig. 5b), but do not see an effect of the drought that ranged from May–August. The EVI values in most other RW sites (mainly within the western part) did not seem to be lower than usual. In comparison to 2003 the heatwave in August 2013 had a more widespread impact, with lower EVI anomaly values occurring across the country (Fig. 5c). Both lower as well as higher located sites seemed to be affected (see elevation map in Fig. 1b). In Fig. 5d a higher located site (i.e. TOB at 821 m.a.s.l.) showed a drop in EVI in the end of August (DOY ~230) but also a fast recovery of the EVI value afterwards. In Fig. 5e, the impact of the February 2014 ice storm is presented. Mainly areas at higher elevation were seriously affected as can be seen in the site VOJ (Fig. 5f). The negative EVI anomaly prevailed across the entire growing season starting around the beginning of May (DOY ~120).

3.3. Trends in beech growth based on RWI and EVI related to climate

Besides the effect of climate extremes, we also investigated the long-term effect of climate change. In Fig. 4 we plotted two of the RWI time-series (ranging from 1961–2016). Both have significant negative RWI trends. This was also the case for quite a few other sites (Appendix C). The sites with NA had too little data (< 5 years) to carry out trend analysis. The remotely sensed EVI data showed negative trends for some sites in specific months (especially June-August – Appendix C). Although the ice storm of 2014 had an impact on the trend analysis of the RWI and EVI (e.g. the site VOJ), many sites with significant negative trends showed a clear decline already before 2014 (e.g. the site VAN).

The monthly EVI data could also be used to assess where EVI has a negative or positive trend for all the regions with beech cover. Fig. 6 shows all significant trends indicating where beech growth could be hampered. The region around the site VOJ is mainly affected by the ice storm in 2014 but we can also observe areas in central Slovenia where beech growth is impeded.

3.4. Linking the RWI and EVI results

Our results indicated that the rise in temperatures and more frequent droughts could have a long term effect on RWI and EVI (i.e. trend analysis - Appendix C – Table C1). We found a significant correlation between RWI (annual) and EVI (average over growing season) for five of the eight sites (these are the sites with a sufficiently long overlapping time-series) (Appendix C – Table C2).

4. Discussion

4.1. The effect of climate extremes on growth of beech in Slovenia

The ring width perspective

We found that years which were extremely dry and/or had extreme high temperatures had in general a lower RWI, especially the years 1993, 2003 and 2011, which is in agreement with results found in other studies (Camarero et al., 2018). However, the large variation within climate classes (Fig. 3) indicates that other factors are at play besides SPI, precipitation and temperature. Another problem are late frost events (e.g. in May 2015) that damage the young leaves in their early stage of development and lead to a great loss of nutrients which is reflected radial growth (Slovenian Forest Service, 2017). Furthermore, we observed a drastic drop in RWI in all sites (Appendix C), especially in sites located in the West of Slovenia at high altitudes (> 1000 m.a.s.l.) as a consequence of the 2014 ice storm, causing serious ecological and economical damage in Slovenia (Marenče, 2015; Slovenian Forest Service, 2017). The RWI values were categorized under 'normal' years when assessing drought or temperatures. This was also the case for (small scale) ice storms in 1980 and 2010, but also other biotic factors such as insect outbreaks and masting years can impact beech tree growth as well (Sinjur et al., 2010; Hacket-Pain et al., 2015; Vacchiano et al., 2017). In general, it is not always easy to identify statistical differences in the relation between climate (extreme) parameters and RWI due to the complexity of the relationship between variables and the different spatial scales at which these interactions can occur. To identify which climate variables at a certain time in the year are affecting RWI is complex and interaction of the variables leads to non-uniform beech stem growth over a great variety of sites (Čufar et al., 2015, 2012, 2008b; Di Filippo et al., 2007; Fischer and Neuwirth, 2013; Prislan et al., 2018, 2013). Site conditions such as soil moisture and altitude can play an important role by limiting the negative effect of drought on wet soils (Gazol et al., 2018, 2017), or lower maximum temperatures on higher altitudes (Čufar et al., 2012; Prislan et al., 2013).

We also found that extreme dry periods in late summer can affect RWI in the following year. In late summer trees invest in building up reserves such as carbohydrates and lipids (Glerum, 1980). Our results are in line with the study by Hacket-Pain et al. (2015), who found reduced RWI in beech after years with high temperatures.
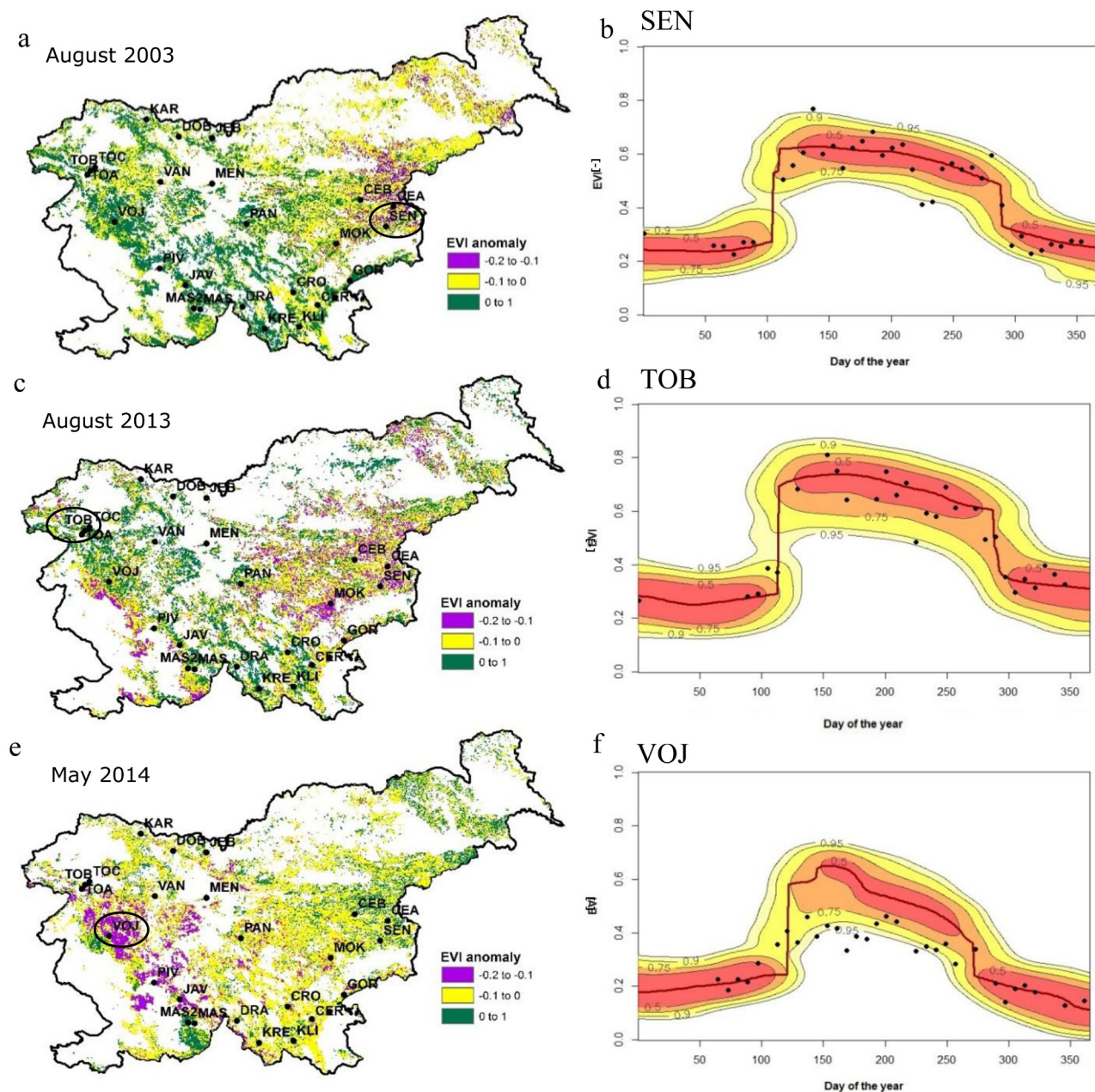
Fig. 5. Left: EVI anomaly maps showing the impact of climate extremes (drought and heatwave in 2003, heatwave in 2013, and ice storm in 2014). Right: EVI anomalies in the selected sites in the corresponding years.

The remote sensing perspective

The results of climate extreme data in Sections 3.1 and 3.2 show that there is no straightforward effect of climate extreme events on remote sensing indices for beech. For example, years with low SPI values (droughts) often resulted in a low RWI, while this was not the case for EVI anomalies. The years with extremely low SPI values seem to have even a positive effect on the canopy. However, focussing on known years with severe climate extremes (i.e. burning of leaves due to hot temperatures) made it feasible to assess effects on EVI anomaly in specific months (Fig. 5). This indicates that climate extremes have to cause physical damage to the trees' canopy before they can be picked up by the EVI anomaly data. Furthermore, some of the lower EVI anomalies might have been caused by late frost events (a parameter that we did not consider in this study).

However, other studies have shown that it is possible to detect and map the impact of droughts and heatwaves on forest canopies with remote sensing indices (Buras et al., 2019; Hlásny et al., 2015). The methods work particularly well when there is a drastic change in the canopy, such as leaf discolouration or even leaf shedding (Buras et al., 2019; Deshayes et al., 2006). Using EVI anomalies, we were able to map and quantify these more drastic and abrupt changes in tree canopies, and through EVI anomalies across the entire growing season we could illustrate the large effect of the ice storm event in 2014 (Fig. 5e,f) affecting in particular the higher elevation in the West of Slovenia. Similar approaches were used to map other large-scale catastrophic events such as wind throw and insect outbreaks (Babst et al., 2010; Coops et al., 2009; Estay et al., 2019). Yet, it will always be difficult to disentangle causes of such canopy disturbances automatically.

Despite the difficulties in capturing more discrete climate effects (i.e. effects not causing obvious physical damage), we observed a generally negative trend in EVI values during the growing season of beech. This was especially the case for sites located in the western part
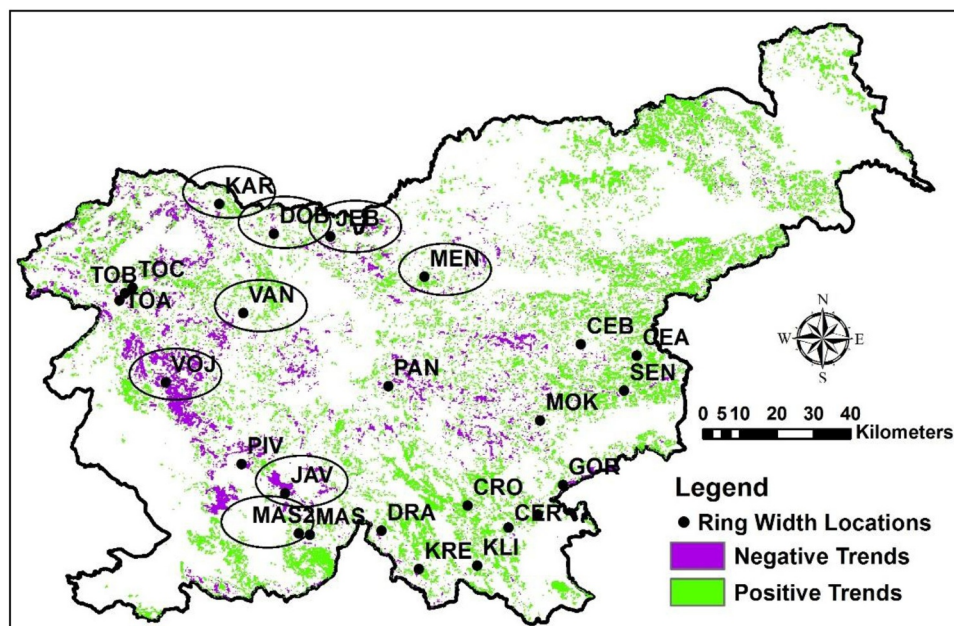
Fig. 6. Beech covered pixels which have significant negative (purple) or positive (green) trends in monthly EVI data over time (2001–2017). Locations with a negative trend in RW between 2001–2016 are indicated by a circle.(For interpretation of the references to colour in this figure legend, the reader is referred to the web version of this article.)

of Slovenia (e.g. DOB, JAV, MAS2, PIV, TOA, VOJ) (Appendix) indicating a decline of photosynthetically active canopy (even before the 2014 ice storm, as the EVI curve was already declining before 2014). This means that the rising temperature and more frequent droughts do affect beech growth in the longer term. The reduction of photosynthesis could cause a drop in carbon uptake and less wood formation (Pinheiro and Chaves, 2010).

4.2. Integration of remote sensing and ring width data

We showed that both space-based and ground-based data contain important information to assess the effect of climate factors, and especially climate extremes on tree growth. The fact that EVI data does not seem to detect climate extreme events, besides physical damage to the canopy, makes the integration of data sources with respect to assessing climate extremes challenging (Norman et al., 2016). However, both RWI and EVI data showed negative trends, and five of the eight sites had a positive correlation. Although more research is needed on linking these two data sources, there are strong indications that the ongoing increase in temperature and decrease in water availability (SPI and precipitation changes) play a role. The increase in temperature and decrease in water availability, together with the higher frequency of extreme climate events could lead to increased beech mortality in the near future. For example, in the north of Spain it was observed that beech forest is declining in the lower altitudinal ranges (Peñuelas et al., 2007). The recent summer drought of 2018, which mainly affected forests in North, Central and East Europe (Buras et al., 2019), has led to beech decline e.g. in Bavaria and Eastern Germany (personal communication Buras, 2019). By mapping beech areas, which based on EVI were sensitive to past climate extremes, we can make predictions on areas that will potentially be most affected by future summer droughts. Here specific climate-smart management tools can be applied to reduce the risk of drought (Sohn et al., 2016).

5. Conclusion

Specific climate extreme events (droughts, high temperatures and ice storms) have an effect on RWI but do not cover all the climatic influences (e.g. spring temperatures and late frosts). Remotely sensed EVI anomaly data was not able to capture extreme drought or high temperature events until physical damage was caused on the canopy.

Therefore, it was able to capture the burning of leaves due to high temperature in 2013 and the ice storm in 2014, but could not capture the 2003 drought in May-July.

Trend analysis of both EVI as RWI data showed declining beech growth, which indicated the negative effects of rising temperatures and this could also be due to the quick succession of climate extreme events in the last 15 years. The remote sensing derived EVI anomaly maps could be useful to detect areas in which beech canopy growth trends are declining, or to map specific events such as ice storms. This information could be useful for mitigation planning by forest managers and policy makers. Further research should focus on the understanding of climate–growth relations at finer time-scales (i.e. intra-annual wood formation data and cambial phenology), and should seek to link them to remote sensing data. The new generation of hyperspectral sensors (e.g. Sentinel-2) and LiDAR based sensors (e.g. GEDI) will offer new opportunities to better link RWI data as they will improve temporal and spatial accuracies.

Data availability

The data and methods will be made available upon request.

Declaration of Competing Interest

Hereby we declare that we do not have any conflict of interest Yours sincerely, Mathieu Decuyper and co-authors

Innovation and Universities. The cooperation among the international partners was supported by the COST Action FP1106, STReESS. The authors thank Sarah Carter for the language editing, and acknowledge the anonymous reviewers for their valuable comments and corrections.

Supplementary materials

Supplementary material associated with this article can be found, in the online version, at doi:10.1016/j.agrformet.2020.107925.

Reference

Avitabile, V., Herold, M., Heuvelink, G.B.M., Lewis, S.L., Phillips, O.L., Asner, G.P., Armston, J., Ashton, P.S., Banin, L., Bayol, N., Berry, N.J., Boeckx, P., Jong, B.H.J., DeVries, B., Girardin, C.A.J., Kearsley, E., Lindsell, J.A., Lopez-Gonzalez, G., Lucas, R., Malhi, Y., Morel, A., Mitchard, E.T.A., Nagy, L., Qie, L., Quinones, M.J., Ryan, C.M., Ferry, S.J.W., Sunderland, T., Laurin, G.V., Gatti, R.C., Valentini, R., Verbeeck, H., Wijaya, A., Willcock, S., 2015. An integrated pan-tropical biomass map using multiple reference datasets. Glob. Chang. Biol. 22, 1406–1420. https://doi.org/10.1111/gcb.13139.

Babst, F., Bodesheim, P., Charney, N., Friend, A.D., Girardin, M.P., Klesse, S., Moore, D.J.P., Seftigen, K., Dietze, M.C., Eckes, A.H., Enquist, B., Frank, D.C., Mahecha, M.D., Poulter, B., Record, S., Trouet, V., Turton, R.H., Zhang, Z., Evans, M.E.K., 2018. When tree rings go global : challenges and opportunities for retro- and prospective insight. Quat. Sci. Rev. 197, 1–20. https://doi.org/10.1016/j.quascirev.2018.07.009.

Babst, F., Esper, J., Parlow, E., 2010. Landsat TM/ETM + and tree-ring based assessment of spatiotemporal patterns of the autumnal moth (*Epirrita autumnata*) in northernmost Fennoscandia. Remote Sens. Environ. 114, 637–646. https://doi.org/10.1016/j.rse.2009.11.005.

Badeck, F.-W., Bondeau, A., Bottcher, K., Doktor, D., Lucht, W., Schaber, J., Sitch, S., 2004. Responses of spring phenology to climate change. New Phytol. 162, 295–309. https://doi.org/10.1111/j.1469-8137.2004.01059.x.

Bates, D., Mächler, M., Bolker, B., Walker, S., 2014. Fitting linear mixed-effects models using lme4. J. Stat. Softw. 67, 1–48. https://doi.org/10.18637/jss.v067.i01.

Bowman, D.M.J.S., Moreira-Muñoz, A., Kolden, C.A., Chávez, R.O., Muñoz, A.A., Salinas, F., González-Reyes, Á., Rocco, R., de la Barrera, F., Williamson, G.J., Borchers, N., Cifuentes, L.A., Abatzoglou, J.T., Johnston, F.H., 2019. Human–environmental drivers and impacts of the globally extreme 2017 Chilean fires. Ambio 48, 350–362. https://doi.org/10.1007/s13280-018-1084-1.

Bréda, N., Huc, R., Granier, A., Dreyer, E., 2006. Temperate forest trees and stands under severe drought : a review of ecophysiological responses, adaptation processes and long-term consequences. Ann. For. Sci. 63, 625–644. https://doi.org/10.1051/forest.

Bunn, A.G., Hughes, M., Kirdyanov, A.V., Losleben, M., Shishov, V.V., Berner, L.T., Oltchev, A., Vaganov, E.A., 2013. Comparing forest measurements from tree rings and a space-based index of vegetation activity in Siberia. Environ. Res. Lett. 8. https://doi.org/10.1088/1748-9326/8/3/035034.

Buras, A., Rammig, A., Zang, C.S., 2019. Quantifying impacts of the drought 2018 on European ecosystems in comparison to 2003. [Preprint]. https://ui.adsabs.harvard.edu/abs/2019arXiv190608605B.

Burnham, K.P., Anderson, D.R., 2002. Model Selection and Multimodel Inference: A Practical Information-Theoretical Approach, 2nd ed. Springer-Verlag, New York.

Camarero, J., Gazol, A., Sangüesa-Barreda, G., Cantero, A., Sánchez-Salguero, R., Sánchez-Miranda, A., Granda, E., Serra-Maluquer, X., Ibáñez, R., 2018. Forest growth responses to drought at short- and long-term scales in Spain: squeezing the stress memory from tree rings. Front. Ecol. Evol. 6, 9. https://doi.org/10.3389/fevo.2018.00009.

Chávez, O.R., Rocco, R., Gutiérrez, G., Dörner, M., Estay, A.S., 2019. A self-calibrated non-parametric time series analysis approach for assessing insect defoliation of broad-leaved deciduous *Nothofagus pumilio* forests. Remote Sens. 11 (2), 204. https://doi.org/10.3390/rs11020204.

Chávez, R.O., Estay, S.A., Riquelme, G., 2017. Npphen. vegetation phenological cycle and anomaly detection. Using Remote Sensing Data.

Ciais, P., Reichstein, M., Viovy, N., Granier, A., Ogée, J., Allard, V., Aubinet, M., Buchmann, N., Bernhofer, C., Carrara, A., Chevallier, F., De Noblet, N., Friend, A.D., Friedlingstein, P., Grünwald, T., Heinesch, B., Keronen, P., Knohl, A., Krinner, G., Loustau, D., Manca, G., Matteucci, G., Miglietta, F., Ourcival, J.M., Papale, D., Pilegaard, K., Rambal, S., Seufert, G., Soussana, J.F., Sanz, M.J., Schulze, E.D., Vesala, T., Valentini, R., 2005. Europe-wide reduction in primary productivity caused by the heat and drought in 2003. Nature 437, 529–533. https://doi.org/10.1038/nature03972.

Cook, E., 1985. A Time Series Analysis Approach to Tree Ring Standardization. University of Arizona, Tucson, Arizona.

Coops, N.C., Wulder, M.A., Iwanicka, D., 2009. Large area monitoring with a MODIS-based disturbance index (DI) sensitive to annual and seasonal variations. Remote Sens. Environ. 113, 1250–1261. https://doi.org/10.1016/j.rse.2009.02.015.

Čufar, K., De Luis, M., Prislan, P., Gričar, J., Črepinšek, Z., Merela, M., Kajfež-Bogataj, L., 2015. Do variations in leaf phenology affect radial growth variations in *Fagus sylvatica*? Int. J. Biometeorol. 59, 1127–1132. https://doi.org/10.1007/s00484-014-0896-3.

Čufar, K., De Luis, M., Saz, M.A., Črepinšek, Z., Kajfež-Bogataj, L., 2012. Temporal shifts in leaf phenology of beech (*Fagus sylvatica*) depend on elevation. Trees 26, 1091–1100. https://doi.org/10.1007/s00468-012-0686-7.

Čufar, K., Luis, M.D.E., Berdajs, E., Prislan, P., 2008a. Main patterns of variability in beech tree-ring chronologies from different sites in Slovenia and their relation to climate glede na klimo Uvod introduction materials and methods material in metode. Zb. gozdarstva Lesar. 87, 123–134.

Čufar, K., Prislan, P., de Luis, M., Gričar, J., 2008b. Tree-ring variation, wood formation and phenology of beech (*Fagus sylvatica*) from a representative site in Slovenia, SE Central Europe. Trees 22, 749–758. https://doi.org/10.1007/s00468-008-0235-6.

Decuyper, M., Chávez, R.O., Copini, P., Sass-Klaassen, U., 2016. A multi-scale approach to assess the effect of groundwater extraction on *Prosopis tamarugo* in the Atacama desert. J. Arid Environ. 131, 25–34. https://doi.org/10.1016/j.jaridenv.2016.03.014.

Deshayes, M., Guyon, D., Jeanjean, H., Stach, N., Jolly, A., Hagolle, O., 2006. The contribution of remote sensing to the assessment of drought effects in forest ecosystems. Ann. For. Sci. 63, 579–595.

Di Filippo, A., Biondi, F., Čufar, K., De Luis, M., Grabner, M., Maugeri, M., Presutti Saba, E., Schirone, B., Piovesan, G., 2007. Bioclimatology of beech (*Fagus sylvatica* L.) in the Eastern Alps: spatial and altitudinal climatic signals identified through a tree-ring network. J. Biogeogr. 34, 1873–1892. https://doi.org/10.1111/j.1365-2699.2007.01747.x.

Estay, S.A., Chávez, R.O., Rocco, R., Gutiérrez, A.G., 2019. Quantifying massive outbreaks of the defoliator moth Ormiscodes amphimone in deciduous *Nothofagus*-dominated southern forests using remote sensing time series analysis. J. Appl. Entomol. 143, 787–796. https://doi.org/10.1111/jen.12643.

Fischer, S., Neuwirth, B., 2013. 2013. Vulnerability of trees to climate events in temperate forests of West Germany. ISRN Forest. 15. https://doi.org/10.1155/2013/201360.

Fonti, P., Heller, O., Cherubini, P., Rigling, A., Arend, M., 2013. Wood anatomical responses of oak saplings exposed to air warming and soil drought. Plant Biol. 15, 210–219. https://doi.org/10.1111/j.1438-8677.2012.00599.x.

Gazol, A., Camarero, J.J., Anderegg, W.R.L., Vicente-Serrano, S.M., 2017. Impacts of droughts on the growth resilience of northern hemisphere forests. Glob. Ecol. Biogeogr. 26, 166–176. https://doi.org/10.1111/geb.12526.

Gazol, A., Camarero, J.J., Vicente-Serrano, S.M., Sánchez-Salguero, R., Gutiérrez, E., de Luis, M., Sangüesa-Barreda, G., Novak, K., Rozas, V., Tíscar, P.A., Linares, J.C., Martín-Hernández, N., Martínez del Castillo, E., Ribas, M., García-González, I., Silla, F., Camisón, A., Génova, M., Olano, J.M., Longares, L.A., Hevia, A., Tomás-Burguera, M., Galván, J.D., 2018. Forest resilience to drought varies across biomes. Glob. Chang. Biol. 24, 2143–2158. https://doi.org/10.1111/gcb.14082.

Giagli, K., Gričar, J., Vavrčík, H., Menšík, L., Gryc, V., 2016. The effects of drought on wood formation in *Fagus sylvatica* during two contrasting years. IAWA J. 37, 332–348. https://doi.org/10.1163/22941932-20160137.

Glerum, C., 1980. Food sinks and food reserves of trees in temperate climates. N. Z. J. For. Sci. 10, 176–185.

Gruber, A., Strobl, S., Veit, B., Oberhuber, W., 2010. Impact of drought on the temporal dynamics of wood formation in *Pinus sylvestris*. Tree Physiol. 30, 490–501. https://doi.org/10.1093/treephys/tpq003.

Hacket-Pain, A.J., Friend, A.D., Lageard, J.G.A., Thomas, P.A., 2015. The influence of masting phenomenon on growth–climate relationships in trees: explaining the influence of previous summers' climate on ring width. Tree Physiol. 35, 319–330. https://doi.org/10.1093/treephys/tpv007.

Hijmans, R.J., van Etten, J., 2012. raster: geographic analysis and modeling with raster data.

Hipel, K.W., McLeod, A.I., 1994. Time Series Modelling of Water Resources and Environmental Systems, 1st ed. Elsevier, Amsterdam, the Netherlands.

Hlásny, T., Barka, I., Sitková, Z., 2015. MODIS-based vegetation index has sufficient sensitivity to indicate stand-level intra-seasonal climatic stress in oak and beech forests. Ann. For. Sci. 109–125. https://doi.org/10.1007/s13595-014-0404-2.

Hollander, M., Wolfe, D.A., 1973. Nonparametric Statistical Methods, 1st ed. John Wiley & Sons, New York.

Huete, A., Didan, K., Miura, T., Rodriguez, E.P., Gao, X., Ferreira, L.G., 2002. Overview of the radiometric and biophysical performance of the MODIS vegetation indices. Remote Sens. Environ. 83, 195–213. https://doi.org/10.1016/S0034-4257(02)00096-2.

Marenče, J., 2015. Meteorological disasters in Slovenian forests - how to approach the restoration in our specific conditions. Glas. Sumar. Fak. 85–96. https://doi.org/10.2298/GSF15S1085M.

McDowell, N., Pockman, W.T., Allen, C.D., Breshears, D.D., Cobb, N., Kolb, T., Plaut, J., Sperry, J., West, A., Williams, D.G., Yepez, E.A., 2008. Mechanisms of plant survival and mortality during drought: why do some plants survive while others succumb to drought? New Phytol. 178, 719–739. https://doi.org/10.1111/j.1469-8137.2008.02436.x.

Mckee, T.B., Doesken, N.J., Kleist, J., 1993. The relationship of drought frequency and duration ot time scales. Eighth Conf. Appl. Climatol. Am. Meteorol. Soc. Anaheim CA 179–186.

Menzel, A., 2002. Phenology: its importance to the global change community. Clim. Change 54, 379–385. https://doi.org/10.1023/A:1016125215496.

Mölder, A., Bernhardt-Römermann, M., Schmidt, W., 2008. Herb-layer diversity in deciduous forests: raised by tree richness or beaten by beech? For. Ecol. Manage. 256, 272–281. https://doi.org/10.1016/j.foreco.2008.04.012.

Nabuurs, G.J., Pussinen, A., Karjalainen, T., Erhard, M., Kramer, K., 2002. Stemwood volume increment changes in European forests due to climate change-A simulation study with the EFISCEN model. Glob. Chang. Biol. 8, 304–316. https://doi.org/10.1046/j.1354-1013.2001.00470.x.

Norman, S.P., Koch, F.H., Hargrove, W.W., 2016. Forest ecology and management review of broad-scale drought monitoring of forests: toward an integrated data mining approach q. For. Ecol. Manage. 380, 346–358. https://doi.org/10.1016/j.foreco.2016.06.027.

Peñuelas, J., Ogaya, R., Boada, M., Jump, A.S., 2007. Migration, invasion and decline:

changes in recruitment and forest structure in a warming-linked shift of European Beech Forest in Catalonia (NE Spain). Ecography (Cop.) 30, 829–837.

Pinheiro, C., Chaves, M.M., 2010. Photosynthesis and drought: can we make metabolic connections from available data? J. Exp. Bot. 62, 869–882. https://doi.org/10.1093/jxb/erq340.

Prislan, P., Cufar, K., De Luis, M., Gricar, J., 2018. Precipitation is not limiting for xylem formation dynamics and vessel development in European beech from two temperate forest sites. Tree Physiol. 38, 186–197. https://doi.org/10.1093/treephys/tpx167.

Prislan, P., Gričar, J., Čufar, K., de Luis, M., Merela, M., Rossi, S., 2019. Growing season and radial growth predicted for *Fagus sylvatica* under climate change. Clim. Change 153, 181–197. https://doi.org/10.1007/s10584-019-02374-0.

Prislan, P., Gričar, J., de Luis, M., Smith, K.T., Čufar, K., 2013. Phenological variation in xylem and phloem formation in *Fagus sylvatica* from two contrasting sites. Agric. For. Meteorol. 180, 142–151. https://doi.org/10.1016/j.agrformet.2013.06.001.

Sass-Klaassen, U., Fonti, P., Cherubini, P., Gričar, J., Robert, E.M.R., Steppe, K., Bräuning, A., 2016. A tree-centered approach to assess impacts of extreme climatic events on forests. Front. Plant Sci. 7, 1069. https://doi.org/10.3389/fpls.2016.01069.

Scharnweber, T., Manthey, M., Criegee, C., Bauwe, A., Schröder, C., Wilmking, M., 2011. Drought matters - Declining precipitation influences growth of *Fagus sylvatica* L. and Quercus robur L. in north-eastern Germany. For. Ecol. Manage. 262, 947–961. https://doi.org/10.1016/j.foreco.2011.05.026.

Serrano-Notivoli, R., Beguería, S., de Luis, M., 2019. STEAD: a high-resolution daily gridded temperature dataset for Spain. Earth Syst. Sci. Data 11, 1171–1188. https://doi.org/10.5194/essd-11-1171-2019.

Serrano-Notivoli, R., de Luis, M., Beguería, S., 2017a. An R package for daily precipitation climate series reconstruction. Environ. Model. Softw. 89, 190–195. https://doi.org/10.1016/j.envsoft.2016.11.005.

Serrano-Notivoli, R., de Luis, Saz, M., Á., M., Beguería, S., 2017b. Spatially based reconstruction of daily precipitation instrumental data series. Clim. Res. 73, 167–186.

Sinjur, I., Kolšek, M., Race, M., Vertačnik, G., 2010. Ice storm in Slovenia in january 2010 [Žled v Sloveniji januarja 2010]. Gozdarski Vestn. 68, 123–130.

Slovenian Forest Service, 2017. Report of Slovenia forest service on forests for the year 2014 [Poročilo Zavoda za Gozdove Slovenije o gozdovih za leto 2014]. Ljubljana, Slovenia.

Sohn, J.A., Saha, S., Bauhus, J., 2016. Potential of forest thinning to mitigate drought stress: a meta-analysis. For. Ecol. Manage. 380, 261–273. https://doi.org/10.1016/j.foreco.2016.07.046.

van der Werf, G.W., Sass-Klaassen, U.G.W., Mohren, G.M.J., 2007. The impact of the 2003 summer drought on the intra-annual growth pattern of beech (*Fagus sylvatica* L.) and oak (*Quercus robur* L.) on a dry site in the Netherlands. Dendrochronologia 25, 103–112. https://doi.org/10.1016/j.dendro.2007.03.004.

Vicca, S., Balzarolo, M., Filella, I., Granier, A., Herbst, M., Knohl, A., Longdoz, B., Mund, M., Nagy, Z., Pintér, K., 2016. Remotely-sensed detection of effects of extreme droughts on gross primary production. Nat. Publ. Gr. 1–13. https://doi.org/10.1038/srep28269.

White, K., Pontius, J., Schaberg, P., 2014. Remote sensing of spring phenology in northeastern forests: a comparison of methods, field metrics and sources of uncertainty. Remote Sens. Environ. 148, 97–107. https://doi.org/10.1016/j.rse.2014.03.017.

Wigley, T.M.L., Briffa, K.R., Jones, P.D., 1984. On the average value of correlated time series, with applications in dendroclimatology and hydrometeorology. J. Clim. Appl. Meteorol 10.1175/1520-0450(1984)023<0201:OTAVOC>2.0.CO;2.

Wu, G., Liu, X., Chen, T., Xu, G., Wang, W., Zeng, X., Zhang, X., 2015. Elevation-dependent variations of tree growth and intrinsic water-use efficiency in Schrenk spruce (*Picea schrenkiana*) in the western Tianshan mountains. China. Front. Plant Sci. 6, 309. https://doi.org/10.3389/fpls.2015.00309.

Nemani, R.R., Keeling, C.D., Hashimoto, H., Jolly, W.M., Piper, S.C., Tucker, C.J., Myneni, R.B., Running, S.W., 2003. Climate-Driven Increases in Global Terrestrial Net Primary Production from 1982 to 1999 300, 1560–1563.